

Source Localization Using Vector Sensor Array in a Multipath Environment

Dayan Rahamim, Joseph Tabrikian, *Senior Member, IEEE*, and Reuven Shavit, *Senior Member, IEEE*

Abstract—Coherent signals from distinct directions is a natural characterization of the multipath propagation effect. This paper addresses the problem of coherent/fully correlated source localization using vector sensor arrays. The maximum likelihood (ML) and minimum-variance distortionless response (MVDR) estimators for source direction-of-arrival (DOA) and signal polarization parameters are derived. These estimators require no search over the polarization parameters. In addition, a novel method for “decorrelating” the incident signals is presented. This method is based on the polarization smoothing algorithm (PSA) and enables the use of eigenstructure-based techniques, which assume uncorrelated or partially correlated signals. The method is implemented as a preprocessing stage before applying eigenstructure-based techniques, such as MUSIC. Unlike other existing preprocessing techniques, such as spatial smoothing and forward-backward (FB) averaging, this method is not limited to any specific array geometry. The performance of the proposed PSA preprocessing combined with MUSIC is evaluated and compared to the Cramér–Rao Bound (CRB) and the ML and MVDR estimators. Simulation results show that the MVDR and PSA-MUSIC asymptotically achieve the CRB for a scenario with two coherent sources with and without an uncorrelated interference source. A sensitivity study of PSA-MUSIC to source polarization was also conducted via simulations.

Index Terms—Coherent sources, electromagnetic vector sensors, maximum-likelihood (ML), multipath, MUSIC, MVDR, polarization smoothing algorithm (PSA), source localization.

I. INTRODUCTION

VECTOR sensors enable estimation of the angle of arrival and polarization of impinging electromagnetic waves with arbitrary polarization. During the last decade, many array processing techniques for source localization and polarization estimation using vector sensors have been developed. Nehorai and Paldi [1], [2] developed the Cramér–Rao bound (CRB) for this problem as well as the vector cross-product direction-of-arrival (DOA) estimator. Polarimetric modeling using vector sensors are presented in [3]. Identifiability and uniqueness issues associated with vector sensors are analyzed in [4]–[8]. Source tracking algorithms using vector sensors have been proposed in [9] and [10].

The maximum likelihood (ML) approach for diversely polarized source localization was proposed in [11]. This method is applicable for both correlated and uncorrelated signals.

Manuscript received March 26, 2003; revised November 10, 2003. The associate editor coordinating the review of this paper and approving it for publication was Dr. Jan C. de Munck.

The authors are with the Department of Electrical and Computer Engineering, Ben-Gurion University of the Negev, Beer Sheva 84105, Israel.

Digital Object Identifier 10.1109/TSP.2004.836456

However, the resulting ML estimator involves a multidimensional optimization procedure over the parameter space, which includes the polarization vector parameters in addition to the DOAs. In order to avoid an exhaustive search procedure of these parameters, a simulated annealing technique was used.

Eigenstructure-based source localization techniques, such as ESPRIT and MUSIC, using vector sensors, have been extensively investigated. Li [12], [13] applied the ESPRIT algorithm to a vector sensor array. ESPRIT-based direction-finding algorithms using vector sensors have been further investigated in several papers [14]–[19]. MUSIC-based algorithms for this problem have been applied in [20]–[22]. Another approach, based on the noise subspace fitting, was suggested in [23]. These techniques yield high-resolution and asymptotically efficient estimates in the case of uncorrelated or partially correlated signals. However, because of the assumption of non-singular signal correlation matrix, these techniques encounter difficulties in cases of coherent/fully correlated signals like in multipath scenarios.

In order to “decorrelate” the signals in the data covariance matrix, Evans *et al.* [24] proposed a preprocessing technique referred to as spatial smoothing. Several authors [25]–[27] investigated this method, combined with forward-backward (FB) averaging. The drawback of this approach is the reduction of the effective array aperture length, resulting in lower resolution and accuracy. An alternative spatial averaging method is redundancy averaging [28], [29]. In [30], it is shown that this preprocessing method induces bias in the DOA estimates.

In this paper, we develop three algorithms for source localization using an array of vector sensors. The ML and minimum-variance distortionless response (MVDR) estimators are derived for DOA and polarization estimation for fully correlated sources. In addition, a novel preprocessing method is proposed to remove the singularity in the signal correlation matrix. The proposed method is based on the polarization smoothing algorithm (PSA), which enables the use of eigenstructure-based algorithms, such as MUSIC and ESPRIT, for DOA estimation in scenarios of fully correlated signals. Unlike the spatial smoothing and FB averaging methods, the PSA preprocessing is not limited to any specific array geometry, and it does not decrease the effective array aperture.

This paper is organized as follows. Section II describes the measurement model using a vector sensor array. The ML and MVDR estimators for DOA and polarization parameters are derived in Section III. Section IV presents the proposed PSA method as a preprocessing stage for eigenstructure-based source localization. The performances of the proposed algorithms are

evaluated via computer simulations and described in Section V. Section VI summarizes our conclusions.

II. PROBLEM FORMULATION AND MODELING

Consider a vector sensor containing three electric and three magnetic orthogonal sensors/dipoles, azimuthally rotated by an angle δ , as depicted in Fig. 1.

The spatial response in matrix notation of the vector sensor can be expressed by

$$\mathbf{g}_0(\theta, \phi, \mathbf{p}) = \underbrace{\begin{bmatrix} -\cos\theta \sin(\phi - \delta) & -\cos(\phi - \delta) \\ \cos\theta \cos(\phi - \delta) & -\sin(\phi - \delta) \\ -\sin\theta & 0 \\ -w \sin(\phi - \delta) & -w \cos\theta \cos(\phi - \delta) \\ -w \cos(\phi - \delta) & w \cos\theta \sin(\phi - \delta) \\ 0 & w \sin\theta \end{bmatrix}}_{\mathbf{A}(\theta, \phi)} \underbrace{\begin{bmatrix} p_\theta \\ p_\phi \end{bmatrix}}_{\mathbf{p}} \quad (1)$$

where w denotes the ratio between the induced voltage in an electric sensor to the corresponding induced voltage in a magnetic sensor. The polarization vector \mathbf{p} is determined by two real parameters γ and η : $p_\theta = \sin\gamma e^{j\eta}$ and $p_\phi = \cos\gamma$. In general, a vector sensor may contain part of the six sensors shown in Fig. 1, and therefore, the corresponding spatial response vector size is given by $1 \leq L \leq 6$.

For the general case of a three-dimensional (3-D) array with N vector sensors, the spatial response in matrix notation of the array vector sensors is expressed by

$$\mathbf{g}(\theta, \phi, \mathbf{p}) = \mathbf{q}(\theta, \phi) \otimes \mathbf{g}_0(\theta, \phi, \mathbf{p}) = \underbrace{[\mathbf{q}(\theta, \phi) \otimes \mathbf{A}(\theta, \phi)]}_{\mathbf{F}(\theta, \phi)} \mathbf{p} \quad (2)$$

where \otimes denotes the Kronecker product. The size of the vector $\mathbf{q}(\theta, \phi)$ is $N \times 1$, and its elements represent the phase delay associated with each vector sensor in the array due to its relative location (x_n, y_n, z_n) for an incident plane wave from the direction (θ, ϕ) :

$$q_n(\theta, \phi) = e^{jk_0[x_n \sin\theta \cos\phi + y_n \sin\theta \sin\phi + z_n \cos\theta]}, \quad n = 1, \dots, N \quad (3)$$

and k_0 is the wavenumber in the medium.

Consider the scenario of M signals, impinging on the array from directions (θ_m, ϕ_m) and polarization vectors \mathbf{p}_m , where $m = 1, \dots, M$. Then, the spatial response of the array to the m th signal is denoted by $\mathbf{g}(\theta_m, \phi_m, \mathbf{p}_m)$, and the data model is given by

$$\begin{aligned} \mathbf{y}_k &= \sum_{m=1}^M \mathbf{g}(\theta_m, \phi_m, \mathbf{p}_m) s_{mk} + \mathbf{n}_k \\ &= \sum_{m=1}^M \mathbf{F}(\theta_m, \phi_m) \mathbf{p}_m s_{mk} + \mathbf{n}_k, \quad k = 1, \dots, K \end{aligned} \quad (4)$$

where K is the number of independent samples collected by the array, and \mathbf{n}_k represents the k th sample of the additive noise and interference vector.

The measurement and noise vectors \mathbf{y}_k and \mathbf{n}_k are each of size LN , the matrix $\mathbf{F}(\theta_m, \phi_m)$ is of size $LN \times 2$, whose

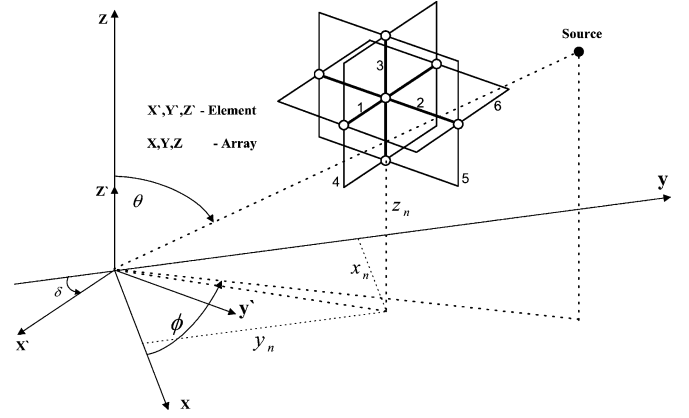


Fig. 1. Vector sensor geometry.

columns denote the spatial transfer functions for both polarization components of the m th signal, and \mathbf{p}_m is a complex vector of size 2, describing the corresponding signal polarization state.

Equation (4) can be rewritten in matrix notation in the form

$$\mathbf{y}_k = \mathbf{F}_T(\theta, \phi) \mathbf{P} \mathbf{s}_k + \mathbf{n}_k, \quad k = 1, \dots, K \quad (5)$$

in which $\mathbf{s}_k \triangleq [s_{1k}, \dots, s_{Mk}]^T$, and the matrices $\mathbf{F}_T(\theta, \phi)$ and \mathbf{P} are defined as

$$\mathbf{F}_T(\theta, \phi) \triangleq [\mathbf{F}(\theta_1, \phi_1) \quad \mathbf{F}(\theta_2, \phi_2) \cdots \mathbf{F}(\theta_M, \phi_M)] \quad (6)$$

$$\mathbf{P} \triangleq \begin{bmatrix} \mathbf{p}_1 & \mathbf{0} & \cdots & \mathbf{0} \\ \mathbf{0} & \mathbf{p}_2 & \cdots & \mathbf{0} \\ \vdots & \vdots & \ddots & \vdots \\ \mathbf{0} & \mathbf{0} & \cdots & \mathbf{p}_M \end{bmatrix}. \quad (7)$$

The sizes of matrices $\mathbf{F}_T(\theta, \phi)$ and \mathbf{P} are $LN \times 2M$ and $2M \times M$, respectively. The signal vector may include both correlated and uncorrelated sources.

The problem addressed in this paper is to estimate the directions of arrival $(\theta, \phi) = (\theta_1, \dots, \theta_M, \phi_1, \dots, \phi_M)$, whereas the signal vectors $(\mathbf{s}_1, \dots, \mathbf{s}_K)$ and the signal polarizations of the M arrivals $(\mathbf{p}_1, \dots, \mathbf{p}_M)$ are unknown complex vector parameters.

III. ML ESTIMATOR

In this section, the ML estimator is derived for coherent source localization using polarized arrays as described above, in the presence of interference sources. Under mild regularity conditions, the ML estimator asymptotically achieves the CRB, as the number of snapshots tends to infinity.

The model for which we derive the ML estimator is

$$\mathbf{y}_k = \sum_{m=1}^M \mathbf{F}(\theta_m, \phi_m) \mathbf{p}_m s_{mk} + \mathbf{n}_k, \quad k = 1, \dots, K \quad (8)$$

where the source signals (s_{1k}, \dots, s_{Mk}) are now considered to be fully correlated, and \mathbf{n}_k represents the other sources and interferences that are not fully correlated with the signals of interest s_{mk} . The noise and interference vectors $\{\mathbf{n}_k\}_{k=1}^K$ are assumed to be i.i.d. with zero-mean, complex Gaussian distribution, $\mathbf{n}_k \sim CN(\mathbf{0}, \mathbf{R}_n)$, and independent of the signals s_{mk} , which are assumed to be unknown deterministic. Since

the signals s_{mk} are assumed to be fully correlated, they can be decomposed as $s_{mk} = \mu_m s_k$, $m = 1, \dots, M$, $k = 1, \dots, K$, where μ_m denotes the relative amplitude and phase of the m th signal. Thus, (8) can be rewritten in the form

$$\mathbf{y}_k = \sum_{m=1}^M \mathbf{F}(\theta_m, \phi_m) \underbrace{\mu_m}_{\zeta_m} s_k + \mathbf{n}_k, \quad k = 1, \dots, K \quad (9)$$

or in short notation as

$$\mathbf{y}_k = \mathbf{F}_T(\boldsymbol{\theta}, \boldsymbol{\phi}) \boldsymbol{\zeta} s_k + \mathbf{n}_k, \quad k = 1, \dots, K \quad (10)$$

where

$$\boldsymbol{\zeta} \triangleq [\zeta_1^T \zeta_2^T \dots \zeta_M^T]^T \quad (11)$$

and $\mathbf{F}_T(\boldsymbol{\theta}, \boldsymbol{\phi})$ is defined in (6).

In the following, two ML estimators for this problem are derived. In the first one, we assume that the noise and interference covariance matrix \mathbf{R}_n is known, while in the second, \mathbf{R}_n is assumed to be unknown and is estimated. In the second case, the likelihood function is related to the MVDR. The resulting estimators in both cases have similar structures.

A. Known Interference Covariance Matrix

In this subsection, we derive the ML estimator for the source directions $(\boldsymbol{\theta}, \boldsymbol{\phi})$, where the modified signal polarization vector $\boldsymbol{\zeta}$ and the signal $\mathbf{s} \triangleq (s_1, \dots, s_K)^T$ are unknown and treated as nuisance parameters. The noise and interference covariance matrix \mathbf{R}_n is assumed to be known.

The ML estimator of the source location is given by

$$(\hat{\boldsymbol{\theta}}, \hat{\boldsymbol{\phi}}) = \arg \max_{\boldsymbol{\theta}, \boldsymbol{\phi}} L_y(\boldsymbol{\theta}, \boldsymbol{\phi}) \quad (12)$$

where $L_y(\boldsymbol{\theta}, \boldsymbol{\phi})$ is the localization function, which is defined as

$$L_y(\boldsymbol{\theta}, \boldsymbol{\phi}) = \max_{\boldsymbol{\zeta}, \mathbf{s}} L_y(\boldsymbol{\theta}, \boldsymbol{\phi}, \boldsymbol{\zeta}, \mathbf{s}) \quad (13)$$

and $L_y(\boldsymbol{\theta}, \boldsymbol{\phi}, \boldsymbol{\zeta}, \mathbf{s}) \triangleq \log f(\mathbf{y}_1, \dots, \mathbf{y}_K | \boldsymbol{\theta}, \boldsymbol{\phi}, \boldsymbol{\zeta}, \mathbf{s})$ is the conditional probability density function (pdf) of the measurements $\mathbf{y}_1, \dots, \mathbf{y}_K$ given the unknown parameters $\boldsymbol{\theta}, \boldsymbol{\phi}, \boldsymbol{\zeta}, \mathbf{s}$.

According to the assumptions stated in the previous section, $\{\mathbf{y}_k\}_{k=1}^K$ is a sequence of independent random vectors $\mathbf{y}_k \sim CN(\boldsymbol{\xi}(\boldsymbol{\theta}, \boldsymbol{\phi}, \boldsymbol{\zeta}) s_k, \mathbf{R}_n)$, where

$$\boldsymbol{\xi} \triangleq \mathbf{F}_T(\boldsymbol{\theta}, \boldsymbol{\phi}) \boldsymbol{\zeta}. \quad (14)$$

Therefore, the log-likelihood function is given by

$$L_y(\boldsymbol{\theta}, \boldsymbol{\phi}, \boldsymbol{\zeta}, \mathbf{s}) = -K \log(\pi |\mathbf{R}_n|) - \sum_{k=1}^K (\mathbf{y}_k - \boldsymbol{\xi}(\boldsymbol{\theta}, \boldsymbol{\phi}, \boldsymbol{\zeta}) s_k)^H \mathbf{R}_n^{-1} (\mathbf{y}_k - \boldsymbol{\xi}(\boldsymbol{\theta}, \boldsymbol{\phi}, \boldsymbol{\zeta}) s_k). \quad (15)$$

The ML estimator of the signal vector \mathbf{s} can be obtained by equating the corresponding derivative of the log-likelihood function to zero, which results in

$$\hat{s}_k = (\boldsymbol{\xi}^H \mathbf{R}_n^{-1} \boldsymbol{\xi})^{-1} \boldsymbol{\xi}^H \mathbf{R}_n^{-1} \mathbf{y}_k. \quad (16)$$

Substitution of (16) into (15) yields

$$L_y(\boldsymbol{\theta}, \boldsymbol{\phi}, \boldsymbol{\zeta}, \hat{\mathbf{s}}) = C + K \frac{\boldsymbol{\xi}^H \mathbf{R}_n^{-1} \hat{\mathbf{R}}_y \mathbf{R}_n^{-1} \boldsymbol{\xi}}{\boldsymbol{\xi}^H \mathbf{R}_n^{-1} \boldsymbol{\xi}} \quad (17)$$

where $\hat{\mathbf{R}}_y = (1/K) \sum_{k=1}^K \mathbf{y}_k \mathbf{y}_k^H$ denotes the sample covariance matrix, and $C \triangleq -K \log(\pi |\mathbf{R}_n|) - \sum_{k=1}^K \mathbf{y}_k^H \mathbf{R}_n^{-1} \mathbf{y}_k$. By denoting

$$\begin{aligned} \boldsymbol{\Psi}_1(\boldsymbol{\theta}, \boldsymbol{\phi}) &\triangleq \mathbf{F}_T^H(\boldsymbol{\theta}, \boldsymbol{\phi}) \mathbf{R}_n^{-1} \mathbf{F}_T(\boldsymbol{\theta}, \boldsymbol{\phi}) \\ \boldsymbol{\Psi}_2(\boldsymbol{\theta}, \boldsymbol{\phi}) &\triangleq \mathbf{F}_T^H(\boldsymbol{\theta}, \boldsymbol{\phi}) \mathbf{R}_n^{-1} \hat{\mathbf{R}}_y \mathbf{R}_n^{-1} \mathbf{F}_T(\boldsymbol{\theta}, \boldsymbol{\phi}) \end{aligned}$$

and substituting the definition $\boldsymbol{\xi} \triangleq \mathbf{F}_T(\boldsymbol{\theta}, \boldsymbol{\phi}) \boldsymbol{\zeta}$, we obtain a simplified form of (17):

$$L_y(\boldsymbol{\theta}, \boldsymbol{\phi}, \boldsymbol{\zeta}, \hat{\mathbf{s}}) = C + K \frac{\boldsymbol{\zeta}^H \boldsymbol{\Psi}_2(\boldsymbol{\theta}, \boldsymbol{\phi}) \boldsymbol{\zeta}}{\boldsymbol{\zeta}^H \boldsymbol{\Psi}_1(\boldsymbol{\theta}, \boldsymbol{\phi}) \boldsymbol{\zeta}}. \quad (18)$$

Maximization of the log-likelihood function in (18) with respect to the modified polarization vector $\boldsymbol{\zeta}$ is equivalent to finding the following maximum generalized eigenvalue and corresponding eigenvector [31]:

$$\boldsymbol{\Psi}_2(\boldsymbol{\theta}, \boldsymbol{\phi}) \mathbf{u} = \lambda \boldsymbol{\Psi}_1(\boldsymbol{\theta}, \boldsymbol{\phi}) \mathbf{u}. \quad (19)$$

Thus, the ML localization function is defined as

$$L_{ML}(\boldsymbol{\theta}, \boldsymbol{\phi}) \triangleq L_y(\boldsymbol{\theta}, \boldsymbol{\phi}, \hat{\boldsymbol{\zeta}}, \hat{\mathbf{s}}) = C + K \lambda_{\max}(\boldsymbol{\Psi}_2(\boldsymbol{\theta}, \boldsymbol{\phi}), \boldsymbol{\Psi}_1(\boldsymbol{\theta}, \boldsymbol{\phi})) \quad (20)$$

where $\lambda_{\max}(\cdot, \cdot)$ and $\mathbf{u}_{\max}(\cdot, \cdot)$ stand for the maximum generalized eigenvalue and the corresponding eigenvector of the matrix pair $(\boldsymbol{\Psi}_2(\boldsymbol{\theta}, \boldsymbol{\phi}), \boldsymbol{\Psi}_1(\boldsymbol{\theta}, \boldsymbol{\phi}))$, respectively.

Finally, the ML estimator of the signal DOAs is given by

$$(\hat{\boldsymbol{\theta}}, \hat{\boldsymbol{\phi}})_{ML} = \arg \max_{\boldsymbol{\theta}, \boldsymbol{\phi}} \lambda_{\max}\{\boldsymbol{\Psi}_2(\boldsymbol{\theta}, \boldsymbol{\phi}), \boldsymbol{\Psi}_1(\boldsymbol{\theta}, \boldsymbol{\phi})\} \quad (21)$$

and the estimate of the polarization vector is given by the corresponding generalized eigenvector

$$\hat{\boldsymbol{\zeta}}_{ML} = \mathbf{u}_{\max}(\boldsymbol{\Psi}_2(\hat{\boldsymbol{\theta}}, \hat{\boldsymbol{\phi}}), \boldsymbol{\Psi}_1(\hat{\boldsymbol{\theta}}, \hat{\boldsymbol{\phi}})). \quad (22)$$

The ML estimate of the signal can now be written as

$$\hat{s}_k = \frac{\hat{\boldsymbol{\zeta}}^H \mathbf{F}_T^H(\hat{\boldsymbol{\theta}}, \hat{\boldsymbol{\phi}}) \mathbf{R}_n^{-1} \mathbf{y}_k}{\hat{\boldsymbol{\zeta}}^H \mathbf{F}_T^H(\hat{\boldsymbol{\theta}}, \hat{\boldsymbol{\phi}}) \mathbf{R}_n^{-1} \mathbf{F}_T(\hat{\boldsymbol{\theta}}, \hat{\boldsymbol{\phi}}) \hat{\boldsymbol{\zeta}}}, \quad k = 1, \dots, K. \quad (23)$$

B. Unknown Interference Covariance Matrix

In this subsection, we derive the ML estimator for the problem stated above, where we assume that the noise and interference covariance matrix \mathbf{R}_n is unknown and needs to be estimated. For this purpose, we apply the results obtained in

[32], in which the ML estimator of $\boldsymbol{\varphi}$ for the following model was derived:

$$\mathbf{y}_k = \mathbf{a}(\boldsymbol{\varphi})s_k + \mathbf{n}_k, \quad k = 1, \dots, K. \quad (24)$$

The signal $\mathbf{s} \triangleq (s_1, \dots, s_K)^T$ is assumed to be unknown deterministic, the noise vectors are i.i.d. with $\mathbf{n}_k \sim \mathcal{CN}(\mathbf{0}, \mathbf{R}_n)$, where $\mathbf{R}_n = \boldsymbol{\Phi} + \sigma_n^2 \mathbf{I}$, and $\boldsymbol{\Phi}$ is an unknown non-negative-definite matrix. The vector $\mathbf{a}(\boldsymbol{\varphi})$ is a known function of $\boldsymbol{\varphi}$. Then, in [32], it is shown that the log-likelihood function for estimating $\boldsymbol{\varphi}$ (after maximization with respect to the nuisance parameters, \mathbf{R}_n, \mathbf{s}) is related to the MVDR beamformer by

$$L_{\mathbf{y}}(\boldsymbol{\varphi}, \hat{\mathbf{s}}, \hat{\mathbf{R}}_n) = \text{const} + K \log \frac{\mathbf{a}^H(\boldsymbol{\varphi})\mathbf{a}(\boldsymbol{\varphi})}{\mathbf{a}^H(\boldsymbol{\varphi})\hat{\mathbf{R}}_y^{-1}\mathbf{a}(\boldsymbol{\varphi})} \quad (25)$$

and the corresponding ML estimator is given by

$$\hat{\boldsymbol{\varphi}} = \arg \max_{\boldsymbol{\varphi}} \frac{\mathbf{a}^H(\boldsymbol{\varphi})\mathbf{a}(\boldsymbol{\varphi})}{\mathbf{a}^H(\boldsymbol{\varphi})\hat{\mathbf{R}}_y^{-1}\mathbf{a}(\boldsymbol{\varphi})} \quad (26)$$

under the assumption that all eigenvalues of the sample covariance matrix $\hat{\mathbf{R}}_y$ are greater than σ_n^2 . If the noise and interference covariance matrix is completely unknown, then σ_n^2 tends to zero, and this assumption is always satisfied since the matrix \mathbf{R}_n is non-negative definite. In our problem, (10) is equivalent to (24), where $\boldsymbol{\varphi}$ is given by $\boldsymbol{\varphi} = (\boldsymbol{\theta}^T, \boldsymbol{\phi}^T, \boldsymbol{\zeta}^T)^T$, and $\mathbf{a}(\boldsymbol{\varphi}) = \mathbf{F}_T(\boldsymbol{\theta}, \boldsymbol{\phi})\boldsymbol{\zeta}$. In this case, (26) can be rewritten in the form

$$(\hat{\boldsymbol{\theta}}, \hat{\boldsymbol{\phi}}, \hat{\boldsymbol{\zeta}})_{MV} = \arg \max_{\boldsymbol{\theta}, \boldsymbol{\phi}, \boldsymbol{\zeta}} \frac{\boldsymbol{\zeta}^H \mathbf{F}_T^H(\boldsymbol{\theta}, \boldsymbol{\phi}) \mathbf{F}_T(\boldsymbol{\theta}, \boldsymbol{\phi}) \boldsymbol{\zeta}}{\boldsymbol{\zeta}^H \mathbf{F}_T^H(\boldsymbol{\theta}, \boldsymbol{\phi}) \hat{\mathbf{R}}_y^{-1} \mathbf{F}_T(\boldsymbol{\theta}, \boldsymbol{\phi}) \boldsymbol{\zeta}}. \quad (27)$$

Maximization of (27) with respect to $\boldsymbol{\zeta}$ can be performed in a similar fashion to the derivation of the ML estimator in the previous subsection. Consequently, the resulting estimator for the signal DOAs $(\boldsymbol{\theta}, \boldsymbol{\phi})$ is given by

$$(\hat{\boldsymbol{\theta}}, \hat{\boldsymbol{\phi}})_{MV} = \arg \max_{\boldsymbol{\theta}, \boldsymbol{\phi}} \lambda_{\max} \{ \boldsymbol{\Gamma}_2(\boldsymbol{\theta}, \boldsymbol{\phi}), \boldsymbol{\Gamma}_1(\boldsymbol{\theta}, \boldsymbol{\phi}) \} \quad (28)$$

and the estimate of the polarization vectors is given by the corresponding generalized eigenvector

$$\hat{\boldsymbol{\zeta}}_{MV} = \mathbf{u}_{\max}(\boldsymbol{\Gamma}_2(\hat{\boldsymbol{\theta}}, \hat{\boldsymbol{\phi}}), \boldsymbol{\Gamma}_1(\hat{\boldsymbol{\theta}}, \hat{\boldsymbol{\phi}})) \quad (29)$$

in which $\boldsymbol{\Gamma}_1(\boldsymbol{\theta}, \boldsymbol{\phi})$ and $\boldsymbol{\Gamma}_2(\boldsymbol{\theta}, \boldsymbol{\phi})$ are redefined as

$$\begin{aligned} \boldsymbol{\Gamma}_1(\boldsymbol{\theta}, \boldsymbol{\phi}) &\triangleq \mathbf{F}_T^H(\boldsymbol{\theta}, \boldsymbol{\phi}) \hat{\mathbf{R}}_y^{-1} \mathbf{F}_T(\boldsymbol{\theta}, \boldsymbol{\phi}) \\ \boldsymbol{\Gamma}_2(\boldsymbol{\theta}, \boldsymbol{\phi}) &\triangleq \mathbf{F}_T^H(\boldsymbol{\theta}, \boldsymbol{\phi}) \mathbf{F}_T(\boldsymbol{\theta}, \boldsymbol{\phi}) \end{aligned}$$

where the signal estimate $\hat{\mathbf{s}}$ is obtained from (23). The MVDR localization function $L_{MV}(\boldsymbol{\theta}, \boldsymbol{\phi})$ is defined as the log-likelihood function after maximization over the nuisance parameters, and it can be written as

$$L_{MV}(\boldsymbol{\theta}, \boldsymbol{\phi}) = \text{const} + K \log \lambda_{\max} \{ \boldsymbol{\Gamma}_2(\boldsymbol{\theta}, \boldsymbol{\phi}), \boldsymbol{\Gamma}_1(\boldsymbol{\theta}, \boldsymbol{\phi}) \}. \quad (30)$$

IV. POLARIZATION SMOOTHING ALGORITHM (PSA)

The ML estimators for the two models discussed above are known to be asymptotically efficient; however, they involve a $2M$ -dimensional search procedure for estimating $(\boldsymbol{\theta}, \boldsymbol{\phi})$. Therefore, when M is large, the above ML estimators are computationally expensive and can be solved numerically, as suggested in [11]. Note that in contrast to [11], the ML estimators derived above do not involve any search procedure over the polarization vectors.

Eigenstructure-based techniques such as MUSIC and ESPRIT are computationally efficient for estimating source directions in a multisource environment. These algorithms assume uncorrelated or partially correlated signals. In this section, we present a preprocessing method that enables the utilization of eigenstructure-based techniques in the presence of fully correlated signals.

The eigenstructure-based techniques for source localization, such as MUSIC, rely on identification of the signal and noise subspaces. In the presence of fully correlated signals, the dimension of the signal subspace is smaller than the number of signals M , and therefore, the signal subspace does not span the M -dimensional subspace of the spatial transfer functions $\mathbf{g}(\theta_1, \phi_1, \mathbf{p}_1), \dots, \mathbf{g}(\theta_M, \phi_M, \mathbf{p}_M)$. In this case, it is required to employ the information on the structure of the spatial transfer function $\mathbf{g}(\theta, \phi, \mathbf{p})$ in order to determine its subspace. Spatial smoothing [24], [33], redundancy averaging [28], [29], and FB averaging [33] techniques utilize the information on the structure of the spatial transfer function in order to estimate this subspace or part of it. The deficiency of the spatial smoothing method is the reduction of the effective array aperture length resulting in lower resolution and accuracy, whereas the deficiency of the redundancy averaging method is that its estimation bias does not vanish asymptotically for a large number of measurements. In addition, both approaches are limited to the case of a linear equally spaced (LES) sensor array with far-field approximation. The FB averaging method assumes a symmetric array, far-field approximation and unequal signal phases at the center of the array.

In the proposed method, the vector sensor information is used in order to determine the subspace spanned by the steering vectors $\mathbf{q}(\theta_1, \phi_1), \dots, \mathbf{q}(\theta_M, \phi_M)$, which enables estimation of DOAs using eigenstructure-based methods, such as MUSIC. This objective can be obtained by the PSA, as described below. By substitution of (2) into (4), the measurement model at the array can be written in the form

In the proposed method, the vector sensor information is used in order to determine the subspace spanned by the steering vectors $\mathbf{q}(\theta_1, \phi_1), \dots, \mathbf{q}(\theta_M, \phi_M)$, which enables estimation of DOAs using eigenstructure-based methods, such as MUSIC. This objective can be obtained by the PSA, as described below.

By substitution of (2) into (4), the measurement model at the array can be written in the form

$$\mathbf{y}_k = \sum_{m=1}^M [\mathbf{q}(\theta_m, \phi_m) \otimes \mathbf{A}(\theta_m, \phi_m)] \mathbf{p}_m s_{mk} + \mathbf{n}_k. \quad (31)$$

If we consider only the sensors of type l ($1 \leq l \leq L$), then the corresponding measurement vector \mathbf{y}_{lk} can be expressed as

$$\mathbf{y}_{lk} = \sum_{m=1}^M [\mathbf{q}(\theta_m, \phi_m) \otimes \mathbf{A}_l(\theta_m, \phi_m)] \mathbf{p}_m s_{mk} + \mathbf{n}_{lk} \quad (32)$$

which can be simplified to

$$\mathbf{y}_{lk} = \sum_{m=1}^M \mathbf{q}(\theta_m, \phi_m) z_{ml} s_{mk} + \mathbf{n}_{lk} \quad (33)$$

where $\mathbf{A}_l(\theta_m, \phi_m)$ is the l th row of the matrix $\mathbf{A}(\theta_m, \phi_m)$, the scalar $z_{ml} = \mathbf{A}_l(\theta_m, \phi_m) \mathbf{p}_m$ denotes the response of the l th type sensor for DOA: θ_m, ϕ_m , and \mathbf{n}_{lk} stands for the corresponding noise vector. This observation implies that each type

of sensor array measurements provides a different linear combination of the vectors $\mathbf{q}(\theta_1, \phi_1), \dots, \mathbf{q}(\theta_M, \phi_M)$, as would be the case for uncorrelated signals. The information acquired by the L different sensor types helps to obtain a measurement space in which the signals are not fully correlated. We utilize this concept in order to span the signal subspace, which is a necessary requirement of the eigenstructure-based algorithms for source localization.

Equation (33) can be rewritten in matrix form as

$$\mathbf{y}_{lk} = \mathbf{Q}(\boldsymbol{\theta}, \boldsymbol{\phi}) \mathbf{Z}_l \mathbf{s}_k + \mathbf{n}_{lk}, k = 1, \dots, K, l = 1, \dots, L \quad (34)$$

where $\mathbf{Q}(\boldsymbol{\theta}, \boldsymbol{\phi}) \triangleq [\mathbf{q}(\theta_1, \phi_1), \dots, \mathbf{q}(\theta_M, \phi_M)]$, and $\mathbf{Z}_l \triangleq \text{diag}(z_{1l}, \dots, z_{Ml})$. Therefore, the covariance matrix of each sensor type is given by

$$\mathbf{R}_{y_l} = E[\mathbf{y}_{lk} \mathbf{y}_{lk}^H] = \mathbf{Q} \mathbf{Z}_l \mathbf{R}_s \mathbf{Z}_l^H \mathbf{Q}^H + \mathbf{R}_{n_l}, l = 1, \dots, L \quad (35)$$

in which $\mathbf{R}_s = E(\mathbf{s} \mathbf{s}^H)$ denotes the signal power, and \mathbf{R}_{n_l} denotes the corresponding noise covariance matrix. In the case of M fully correlated signals, the signal covariance matrix of each sensor array type $\mathbf{Q} \mathbf{Z}_l \mathbf{R}_s \mathbf{Z}_l^H \mathbf{Q}^H$ is of rank one. In the proposed PSA, the covariance matrices $\{\mathbf{R}_{y_l}\}_{l=1}^L$ are smoothed for the L elements of the vector sensor. Consequently, the signal subspace is extended by averaging the L sensor-type covariance matrices, i.e.,

$$\mathbf{R} = \frac{1}{L} \sum_{l=1}^L \mathbf{R}_{y_l} = \mathbf{Q} \mathbf{R}_z \mathbf{Q}^H + \frac{1}{L} \sum_{l=1}^L \mathbf{R}_{n_l} \quad (36)$$

in which \mathbf{R}_z is defined as $\mathbf{R}_z \triangleq (1/L) \sum_{l=1}^L \mathbf{Z}_l \mathbf{R}_s \mathbf{Z}_l^H$. The smoothed sample covariance matrix $\hat{\mathbf{R}} = (1/KL) \sum_{l=1}^L \sum_{k=1}^K \mathbf{y}_{lk} \mathbf{y}_{lk}^H$ can be used by eigenstructure-based techniques such as MUSIC, ESPRIT, etc., with the steering vector $\mathbf{q}(\boldsymbol{\theta}, \boldsymbol{\phi})$.

The rank of the smoothed signal covariance matrix $\mathbf{Q} \mathbf{R}_z \mathbf{Q}^H$ is limited by $\min(\text{rank}(\mathbf{R}_z), N)$. Since $\text{rank}(\mathbf{R}_z) \leq \min(L, M)$, then

$$\text{rank}(\mathbf{Q} \mathbf{R}_z \mathbf{Q}^H) \leq \min(L, M, N) \leq \min(L, M). \quad (37)$$

For eigenstructure-based techniques, it is required that

$$\text{rank}(\mathbf{R}) = \text{rank}(\mathbf{Q} \mathbf{R}_z \mathbf{Q}^H) = M. \quad (38)$$

The requirement in (38) and the limitation in (37) imply the constraint $M \leq L$. In addition, in eigenstructure-based techniques, it is required that $M \leq N - 1$. Combining these two constraints yields

$$M \leq \min(L, N - 1). \quad (39)$$

This constraint can be eased if one uses other methods for signal "decorrelation." For example, by applying the FB averaging [25], the maximum number of the fully correlated signals, which can be localized, is doubled. This observation can be justified by noting that in FB-averaging, (36) is modified to $\mathbf{R} = (1/L) \sum_{l=1}^L (\mathbf{R}_{y_l}^F + \mathbf{R}_{y_l}^B)/2$, and based on (36) and (37), the rank of \mathbf{R} satisfies

$$\text{rank}(\mathbf{R}) \leq \text{rank} \left(\sum_{l=1}^L \mathbf{R}_{y_l}^F \right) + \text{rank} \left(\sum_{l=1}^L \mathbf{R}_{y_l}^B \right) \leq \min(2L, 2M). \quad (40)$$

From the constraints (38) and (40), we obtain $M \leq 2L$. Combining this requirement and the eigenstructure-based technique limitation ($M \leq N - 1$) results in the requirement

$$M \leq \min(2L, N - 1) \quad (41)$$

which is an improvement beyond the condition derived in (39).

As shown above, the PSA technique averages the data covariance matrix along the elements in the vector sensors of the array, whereas in the spatial smoothing technique, the averaging operation is performed along the array aperture. Accordingly, the PSA has the following advantages on the spatial smoothing technique:

- There is no limit on the array geometry.
- The array aperture is not decreased.

The vector sensor array contains NL sensors, and therefore, NL receivers are required for data collection. However, the PSA computes the smoothed covariance matrix by averaging the $N \times N$ matrices $\{\mathbf{R}_{y_l}\}_{l=1}^L$. In stationary scenarios, these matrices can be calculated in different periods. This implies that by an appropriate switching scheme [34], [35], one can use N receivers in order to collect the required data.

V. SIMULATION RESULTS

In this section, we evaluate the performance of the proposed techniques for different scenarios. The CRB for source localization using a vector sensor array was derived in [2] and calculated for the scenarios presented below. For the simulations, a five-element linear array of dual polarized vector sensors (see sensors 1 and 3 in Fig. 1 with $\delta = 0^\circ$) along the y-axis with half-wavelength interelement spacing was chosen. The methods evaluated in this section assume zero elevation incident angle ($\theta_m = 90^\circ$) for all sources.

Two scenarios are considered for comparison between the performances of the algorithms. In the first scenario, two equal power, fully correlated sources with DOA azimuth angles $\boldsymbol{\phi} = (20^\circ, 0^\circ)$ and elliptical polarizations, $\mathbf{p}_1 = (0.5e^{j100^\circ}, 0.866)$, $\mathbf{p}_2 = (0.866e^{-j30^\circ}, 0.5)$ were considered. The phase difference between the two incident signals at the origin was 260° such that $\boldsymbol{\zeta}_1 = (0.5, 0.866e^{j260^\circ})$, $\boldsymbol{\zeta}_2 = (0.866e^{-j30^\circ}, 0.5)$. The number of samples taken from the array was $K = 100$. In the second scenario, an uncorrelated interference source was added with the following specifications: DOA azimuth angle $\phi_3 = 40^\circ$ and polarization $\mathbf{p}_3 = \mathbf{p}_1$.

Figs. 2 and 3 show a comparison between the performances of the ML, MVDR, MUSIC, PSA-MUSIC methods, and the CRB. The performance is evaluated by the root-mean-square error (RMSE) of the first source DOA estimation versus signal-to-noise ratio (SNR), where SNR is defined as $\text{SNR} = (1/K) \sum_{k=1}^K |s_k|^2 / \sigma_n^2$. The implemented ML and MVDR methods involve two-dimensional (2-D) search procedures over the DOA paths of the source of interest, whereas in MUSIC and PSA-MUSIC, a one-dimensional (1-D) search is conducted. Fig. 2 refers to the first scenario in which no interference source exists, and therefore, the noise and interference covariance matrix \mathbf{R}_n is equal to $\sigma_n^2 \mathbf{I}$, where $\sigma_n^2 = 1$ is the noise variance at each sensor. One can observe that all the estimators except MUSIC achieve the CRB. The ML and MVDR estimators are superior to the PSA-MUSIC at low SNRs, but they are computationally extensive. Fig. 3 refers

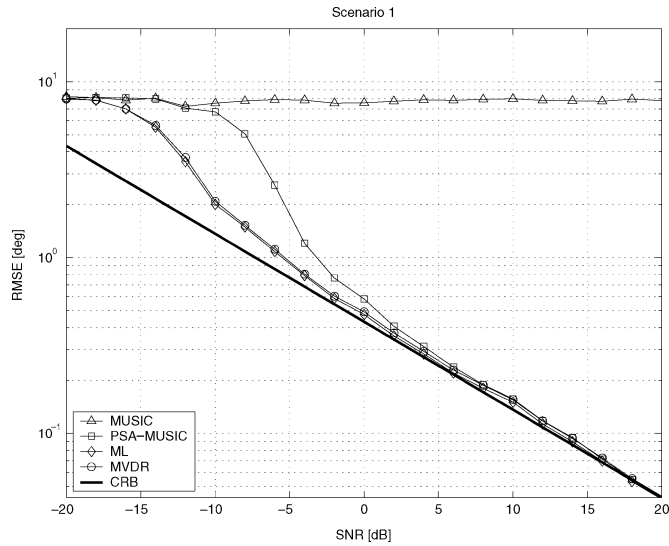


Fig. 2. DOA estimation RMSE versus SNR.

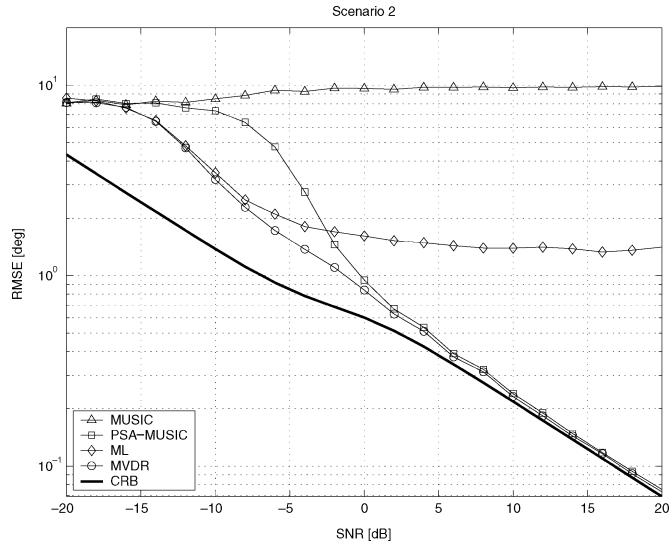


Fig. 3. DOA estimation RMSE versus SNR in the presence of an uncorrelated interference.

to the second scenario, which includes an uncorrelated interference source in addition to the two fully correlated sources. In this case, the noise and interference covariance matrix is given by $\mathbf{R}_n = \sigma_n^2 (\mathbf{I} + \text{INR} \cdot \mathbf{g}(\theta_3, \phi_3, \mathbf{p}_3) \mathbf{g}^H(\theta_3, \phi_3, \mathbf{p}_3))$, where $\mathbf{g}(\cdot, \cdot, \cdot)$ is given in (2), and INR denotes the interference-to-noise ratio, which is defined as $\text{INR} = E(|s_{3k}|^2) / \sigma_n^2$. The INR was chosen to be equal to the SNR. This figure shows that the MVDR and the PSA-MUSIC achieve the CRB in the presence of unknown interference, whereas the RMSE of the ML estimator approaches a constant level when the SNR tends to infinity. The reason for this behavior is that the implemented ML estimator ignores the existence of the uncorrelated interference source. In other words, there is a mismatch in the noise and interference covariance matrix. On the other hand, the MVDR is obtained by derivation of the ML estimator for the model in which the matrix \mathbf{R}_n is unknown and estimated. The plain MUSIC method fails as in the previous scenario.

Fig. 4 shows the log-likelihood functions $L_{ML}(\boldsymbol{\theta}, \boldsymbol{\phi})$ and $L_{MV}(\boldsymbol{\theta}, \boldsymbol{\phi})$ from (20) and (30) for the two scenarios discussed

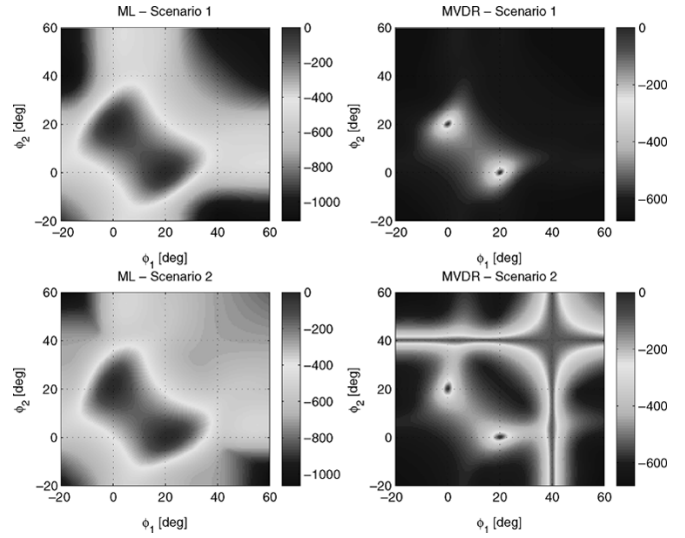


Fig. 4. Normalized log-likelihood functions with and without uncorrelated interference.

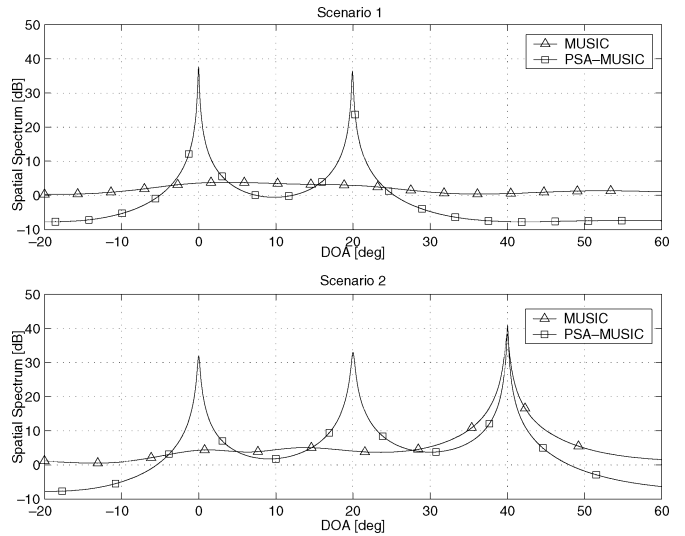


Fig. 5. Spatial spectrum of plain MUSIC and PSA-MUSIC with and without uncorrelated interference.

above with $\text{SNR} = 20$ dB. One can observe that in the first scenario, distinct peaks around the true source locations are identified in the ML and MVDR localization functions. In each figure, two peaks are obtained because of the symmetry in the localization function with respect to ϕ_1 and ϕ_2 . In the second scenario, with $\text{SNR} = \text{INR} = 20$ dB, the peaks in the ML localization function are slightly shifted due to the mismatch in \mathbf{R}_n . In addition, the interference signal is not detected in this case. On the other hand, the MVDR successfully detects both the coherent and the interference sources.

Fig. 5 shows the spatial spectrum functions of the MUSIC and PSA-MUSIC for the scenarios stated above with $\text{SNR} = 20$ dB. One can observe that in the first scenario, distinct peaks around the true source DOAs are identified in the PSA-MUSIC, whereas the plain-MUSIC fails. In the second scenario, in the presence of an uncorrelated interference source, with $\text{SNR} = \text{INR} = 20$ dB, the PSA-MUSIC is able to locate both the coherent and incoherent signals. On the other hand, the plain MUSIC fails to locate the coherent signals.

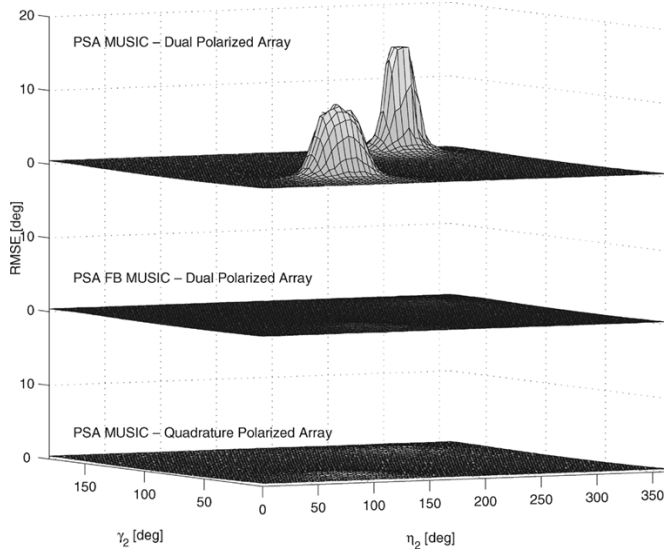


Fig. 6. DOA estimation RMSE versus polarization vector parameters.

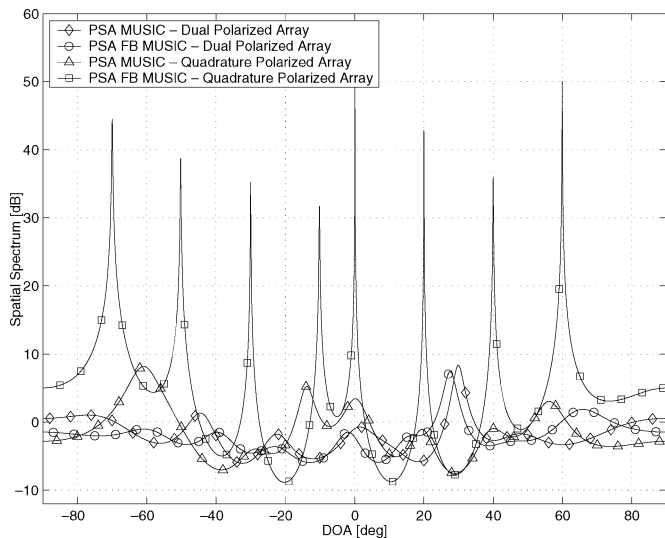


Fig. 7. Spatial spectrum of MUSIC with PSA and PSA-FB preprocessing and vector sensor structures with eight fully correlated sources at -70° , -50° , -30° , -10° , 0° , 20° , 40° , and 60° .

In the next example, the robustness of PSA-MUSIC to signal polarization parameters is evaluated. Two types of arrays were considered: a) Dual polarized array, as in the previous example, and b) quadrature polarized array (see sensors 1, 2, 4, and 5 in Fig. 1 with $\delta = 45^\circ$). The vector sensors consist of two electric dipoles and two magnetic dipoles with $w = 1$ in (1). Scenario 1 was considered with an SNR of 10 dB. The RMSE of the first source DOA estimation versus the signal polarization parameters of the second source (γ_2 and η_2) is depicted in Fig. 6. One can observe that the PSA-MUSIC with dual polarization sensors fails in two polarization cases in which $\mathbf{g}_0(\theta_1, \phi_1, \mathbf{p}_1) = \mathbf{g}_0(\theta_2, \phi_2, \mathbf{p}_2)$ [see (1)]. This deficiency can be solved either by applying FB averaging in addition to PSA-MUSIC or by using a higher order polarized array such as array of type B, as introduced above. The RMSEs of the two cases as a function of polarization appear in the two other surface plots in Fig. 6. These plots show that the RMSEs of the two cases are insensitive to the signal polarization.

Fig. 7 presents the spatial spectrum of the MUSIC algorithm for the two types of arrays used in the previous example for PSA-MUSIC and PSA-FB-MUSIC. The array in this scenario was comprised of $N = 10$ elements of vector sensors. Eight equal power, fully correlated sources with DOAs -70° , -50° , -30° , -10° , 0° , 20° , 40° , 60° , and randomly chosen polarizations were considered. The SNRs of all the signals were 20 dB. This figure shows that in this case only, the PSA-FB-MUSIC with quadrature vector sensor array ($L = 4$) successfully resolves the eight fully correlated signals, as stated in (41): $\min(2L, N - 1) = 8$.

VI. CONCLUSIONS

In this paper, the problem of fully correlated source localization, characterizing multipath scenarios, using a vector sensor array was addressed. The ML and MVDR estimators for source DOA and polarization were derived. The resulting estimators do not require any search over the polarization parameters space. In addition, a novel preprocessing method based on the polarization smoothing algorithm (PSA) for “decorrelating” the signals was presented. This method enables the use of eigenstructure-based techniques, such as MUSIC, for fully correlated signals. In contrast to other preprocessing methods, such as spatial smoothing, forward-backward averaging, and redundancy averaging, the PSA is not limited to any specific array structure. By combining the PSA and forward-backward averaging, one is able to resolve up to $\min(2L, N - 1)$ coherent sources, where L is the number of elements in each of the N vector sensors in the array. Simulations were carried out to evaluate the performance of the proposed methods: ML, MVDR, and PSA-MUSIC for coherent source localization with and without an uncorrelated interference source.

REFERENCES

- [1] A. Nehorai and E. Paldi, “Vector-sensor array processing for electromagnetic source localization,” in *Proc. 25th Asilomar Conf. Signals Syst. Comput.*, Pacific Grove, CA, Nov. 1991, pp. 566–572.
- [2] —, “Vector-sensor array processing for electromagnetic source localization,” *IEEE Trans. Signal Processing*, vol. 42, pp. 376–398, Feb. 1994.
- [3] B. Hochwald and A. Nehorai, “Polarimetric modeling and parameter estimation with application to remote sensing,” *IEEE Trans. Signal Processing*, vol. 43, pp. 1923–1935, Aug. 1995.
- [4] G. F. Hatke, “Conditions for unambiguous source localization using polarization diverse array,” in *Proc. 27th Asilomar Conf.*, 1993, pp. 1365–1369.
- [5] K. C. Ho, K. C. Tan, and W. Ser, “Investigation on number of signals whose directions-of-arrival are uniquely determinable with an electromagnetic vector sensor,” *Signal Process.*, vol. 47, pp. 41–54, Nov. 1995.
- [6] B. Hochwald and A. Nehorai, “Identifiability in array processing models with vector-sensor applications,” *IEEE Trans. Signal Processing*, vol. 44, pp. 83–95, Jan. 1996.
- [7] K. C. Tan, K. C. Ho, and A. Nehorai, “Uniqueness study of measurements obtainable with arrays of electromagnetic vector sensors,” *IEEE Trans. Signal Processing*, vol. 44, pp. 1036–1039, Apr. 1996.
- [8] —, “Linear independence of steering vectors of an electromagnetic vector sensor,” *IEEE Trans. Signal Processing*, vol. 44, pp. 3099–3107, Dec. 1996.
- [9] C. C. Ko, J. Zhang, and A. Nehorai, “Separation and tracking of multiple broadband sources with one electromagnetic vector sensor,” *IEEE Trans. Aerosp. Electron. Syst.*, vol. 38, pp. 1109–1116, July 2002.
- [10] A. Nehorai and P. Tichavsky, “Cross-product algorithms for source tracking using an EM vector sensor,” *IEEE Trans. Signal Processing*, vol. 47, pp. 2863–2867, Oct. 1999.

- [11] I. Ziskind and M. Wax, "Maximum likelihood localization of diversely polarized sources by simulated annealing," *IEEE Trans. Antennas Propagat.*, vol. 38, pp. 1111–1114, July 1990.
- [12] J. Li and R. T. Compton Jr., "Angle and polarization estimation using ESPRIT with a polarization sensitive array," *IEEE Trans. Antennas Propagat.*, vol. 39, pp. 1376–1383, Sept. 1991.
- [13] J. Li, "Direction and polarization estimation using arrays with small loops and short dipoles," *IEEE Trans. Antennas Propagat.*, vol. 41, pp. 379–387, Mar. 1993.
- [14] K. T. Wong and M. D. Zoltowski, "Closed-form direction-finding with arbitrarily spaced electromagnetic vector-sensors at unknown locations," *IEEE Trans. Antennas Propagat.*, vol. 48, pp. 671–681, May 2000.
- [15] M. D. Zoltowski and K. T. Wong, "ESPRIT-based 2-D direction finding with a sparse uniform array of electromagnetic vector sensors," *IEEE Trans. Signal Processing*, vol. 48, pp. 2195–2204, Aug. 2000.
- [16] K. T. Wong, "Blind beamforming/geolocation for wideband-FFH's with unknown hop-sequences," *IEEE Trans. Aerosp. Electron. Syst.*, vol. 37, pp. 65–76, Jan. 2001.
- [17] K. C. Ho, K. C. Tan, and B. T. G. Tan, "Efficient method for estimation of direction-of-arrival of partially polarized signals with electromagnetic vector sensors," *IEEE Trans. Signal Processing*, vol. 45, pp. 2485–2498, Oct. 1997.
- [18] K. C. Ho, K. C. Tan, and A. Nehorai, "Estimating directions of arrival of completely and incompletely polarized signals with electromagnetic vector sensors," *IEEE Trans. Signal Processing*, vol. 47, pp. 2845–2852, Oct. 1999.
- [19] K. T. Wong and M. D. Zoltowski, "Uni-vector-sensor ESPRIT for multi-source azimuth, elevation, and polarization estimation," *IEEE Trans. Antennas Propagat.*, vol. 45, pp. 1467–1474, Oct. 1997.
- [20] —, "Self-initiating MUSIC-based direction finding and polarization estimation in spatio-polarizational beamspace," *IEEE Trans. on Antennas Propagat.*, vol. 48, pp. 1235–1245, Aug. 2000.
- [21] M. D. Zoltowski and K. T. Wong, "Closed-form eigenstructure-based direction finding using arbitrary but identical subarray on a sparse uniform Cartesian array grid," *IEEE Trans. Signal Processing*, vol. 48, pp. 2205–2210, Aug. 2000.
- [22] P. H. Chua, C. M. S. See, and A. Nehorai, "Vector-sensor array processing for estimating angles and times of arrival of multipath communication signals," in *Proc. ICASSP*, vol. 6, May 1998, pp. 3325–3328.
- [23] A. Swindlehurst and M. Viberg, "Subspace fitting with diversely polarized antenna arrays," *IEEE Trans. Antennas Propagat.*, vol. 41, pp. 1687–1694, Dec. 1993.
- [24] J. E. Evans, J. R. Johnson, and D. F. Sun, "High resolution angular spectrum estimation techniques for terrain scattering analysis and angle of arrival estimation," in *Proc. 1st ASSP Workshop Spectral Estim.*, Hamilton, ON, Canada, 1981, pp. 134–139.
- [25] S. U. Pillai and B. H. Kwon, "Forward/backward spatial smoothing techniques for coherent signal identification," *IEEE Trans. Acoust., Speech, Signal Processing*, vol. 37, pp. 8–15, Jan. 1989.
- [26] J. S. Thompson, P. M. Grant, and B. Mulgrew, "Performance of spatial smoothing algorithms for correlated sources," *IEEE Trans. Signal Processing*, vol. 44, pp. 1040–1046, Apr. 1996.
- [27] J. Li, "Improved angular resolution for spatial smoothing techniques," *IEEE Trans. Signal Processing*, vol. 40, pp. 3078–3081, Dec. 1992.
- [28] D. A. Linebarger and D. H. Johnson, "The effect of spatial averaging on spatial correlation matrices in the presence of coherent signals," *IEEE Trans. Acoust., Speech, Signal Processing*, vol. 38, pp. 880–884, May 1990.
- [29] L. C. Godara, "Beamforming in the presence of correlated arrivals using structured correlation matrix," *IEEE Trans. Acoust., Speech, Signal Processing*, vol. 38, pp. 1–15, Jan. 1990.
- [30] K. C. Indukumar and V. U. Reddy, "A note on redundancy averaging," *IEEE Trans. Signal Processing*, vol. 40, pp. 466–469, Feb. 1992.
- [31] R. Schmidt, "A Signal Subspace Approach to Multiple Emitter Location and Spectral Estimation," Ph.D. dissertation, Stanford Univ., Stanford, CA, 1981.
- [32] K. Harmanci, J. Tabrikian, and J. L. Krolik, "Relationships between adaptive minimum variance beamforming and optimal source localization," *IEEE Trans. Signal Processing*, vol. 48, pp. 1–12, Jan. 2000.
- [33] J. E. Evans, J. R. Johnson, and D. F. Sun, "Application of advanced signal processing techniques to angle of arrival estimation in ATC navigation and surveillance systems," MIT Lincoln Lab., Tech. Rep., Lexington, MA, 1982.
- [34] J. Sheinvald and M. Wax, "Direction finding with fewer receivers via time-varying preprocessing," *IEEE Trans. Signal Processing*, vol. 47, pp. 2–9, Jan. 1999.
- [35] J. Tabrikian and A. Faizakov, "Optimal preprocessing for source localization by fewer receivers than sensors," in *Proc. 11th IEEE Signal Processing Workshop Statistical Signal Processing*, 2001, pp. 213–216.



Dayan Rahamim was born in Beer-Sheva, Israel, in October 1969. He received the B.Sc. degree *magna cum laude* in electrical engineering in 1997 and the M.Sc. degree *magna cum laude* in 2003, both from the Ben-Gurion University of the Negev, Beer-Sheva. He is currently Head of the R&D Department, Telrad Networks, Rosh Ha'ayin, Israel, specializing in smart antenna technologies.



Joseph Tabrikian (S'89–M'97–SM'98) received the B.Sc., M.Sc., and Ph.D. degrees in electrical engineering from the Tel-Aviv University, Tel-Aviv, Israel, in 1986, 1992, and 1997, respectively.

From 1992 to 1996, he was a Research and Teaching Assistant with the Department of Electrical Engineering—Systems, Tel-Aviv University. From 1996 to 1998, he was with the Department of Electrical and Computer Engineering, Duke University, Durham, NC, as an Assistant Research Professor.

He is now a Faculty member with the Department of Electrical and Computer Engineering, Ben-Gurion University of the Negev, Beer-Sheva, Israel. His research interests include statistical signal processing, source detection and localization, and speech and audio processing.

Dr. Tabrikian has served as an Associate Editor for the *IEEE TRANSACTIONS ON SIGNAL PROCESSING* since 2001.



Reuven Shavit (M'82–SM'90) was born in Romania on November 14, 1949. He received the B.Sc. and M.Sc. degrees in electrical engineering from the Technion—Israel Institute of Technology, Haifa, Israel, in 1971 and 1977, respectively, and the Ph.D. degree in electrical engineering from the University of California, Los Angeles, in 1982.

From 1971 to 1993, he was a Staff Engineer and Antenna Group Leader with the Electronic Research Laboratories of the Israeli Ministry of Defense, Tel-Aviv, where he was involved in the design of reflector, microstrip, and slot antenna arrays. He was also a part-time lecturer at Tel-Aviv University, teaching various antenna and electromagnetic courses. From 1988 to 1990, he was associated with ESSCO, Concord, MA, as a Principal Engineer, where he was involved in scattering analysis and tuning techniques of high-performance ground-based radomes. Currently, he is with Ben-Gurion University of the Negev, Beer Sheeva, Israel, as a senior lecturer, doing research in microwave components and antennas. His present research interest is in the areas of tuning techniques for radomes, numerical methods for printed antennas, and smart antenna algorithms.